


# Improved resolution Fourier ptychography scheme using oil-filled dome-shaped LED array

Mahdieh Gholami Mayani,<sup>1,✉</sup> Nazabat Hussain,<sup>1</sup> Dag Werner Breiby,<sup>2</sup> and Muhammad Nadeem Akram<sup>1</sup>   
<sup>1</sup>Department of Microsystems, University of South-Eastern Norway (USN), Vestfold Campus, Borre, 3184, Norway  
<sup>2</sup>Department of physics, Norwegian University of Science and Technology (NTNU), Norway

✉ Email: gholamimah@gmail.com

Utilising angular-varied illumination in Fourier Ptychography, the resolution of optical microscopes can be increased and the phase of the sample can also be recovered while maintaining a wide field-of-view. In this work, an Fourier Ptychography microscopy imaging setup is demonstrated using a 10X 0.28 NA objective lens and a dome-shaped light-emitting diode array illuminator. By increasing the refractive index of the medium between the sample and light sources using oil filled dome, a synthetic system numerical aperture of 0.68 is achieved using only 37 light-emitting diodes. The measured resolution of 345 nm at a wavelength of 530 nm closely matches the theoretical prediction. Furthermore, the results of the oil-medium illumination are compared to free-space illumination. The oil immersion on the illumination side effectively enhances the illumination numerical aperture as compared to air and reduces the need for far off-axis light-emitting diodes. The result is high-resolution Fourier Ptychography imaging with relatively fewer light-emitting diodes providing both short capture and reconstruction times.

**Introduction:** Demand for microscopes with high resolving power is steadily increasing in biomedical and pathological applications. In conventional microscope, resolution is mainly limited by the numerical aperture (NA) of its microscope objective lens (OL) that behaves like a low-pass filter with a spatial cutoff frequency. This fundamental constraint restricts the resolution of the system [1]. In case of employing a higher NA OL for better resolution, the image field of view (FOV) gets more restricted as well as requiring a short working distance which can lead to impractical setups and/or sample contamination. Furthermore, optical aberrations, short depth of field (DOF) and no access to the sample phase are shortcomings of current microscopes. Fourier Ptychography microscopy (FPM) is a promising approach to obtain a high synthetic NA while maintaining a wide FOV, additionally retrieving the unknown phase information of the complex object [2–5]. This technique has mainly provenience in conventional ptychography [6], synthetic aperture imaging [7], and structured-illumination imaging [8]. FPM is based on a light-emitting diode (LED) array providing angularly varying coherent illumination on the sample whilst a sequence of images are captured by a digital camera. The captured images are spatially discretely sampled by the camera and the maximum un-aliased spatial frequency is defined according to the Nyquist sampling frequency. By illuminating the sample with off-axis LEDs, assuming a plane-wave illumination, the object spectrum is shifted in the Fourier plane. Thus, numerous subparts of this spectrum consisting of higher spatial frequency information are collected, effectively circumventing the diffraction limit of the corresponding optical system. Because the camera records the squared absolute value of the electric field, a phase recovery algorithm must be applied to the captured images, referred to as low-resolution (LR) images, if the phase information is to be regained. The imaging scheme is carried out by first capturing sequentially the low-resolution images and subsequently improving the complex extended Fourier spectrum in an iterative back-and-forth numerical propagation of the electric field between the camera plane and the Fourier plane. After convergence, the retrieved extended complex Fourier spectrum provides the high spatial resolution (HR) complex sample image.

In FPM, the synthesised NA ( $NA_{synth}$ ) is equal to the sum of the NA of the OL ( $NA_{obj}$ ) and illumination NA ( $NA_{illum}$ ) [2]. The  $NA_{illum}$  is defined as  $n \sin \theta_{max}$  where  $n$  is the refractive index of the medium between the LED sources and the sample, and  $\theta_{max}$  is the largest LED illumination

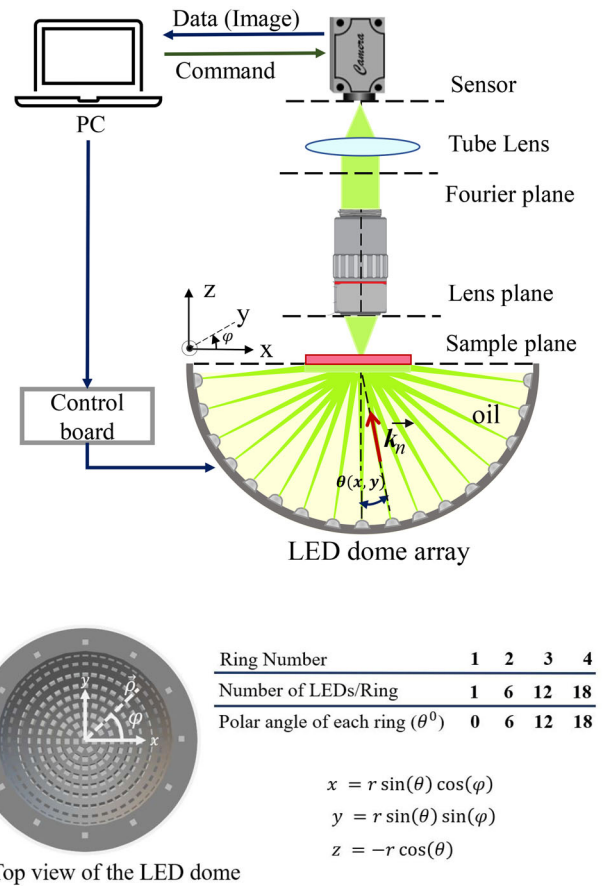


**Fig. 1** Schematic diagram of the FPM experimental setup. Measurements were done with and without having oil in the dome

angle. As  $NA_{obj}$  is pre-determined by the OL, FPM can effectively increase the system NA beyond this restriction. Several attempts have been made to improve the resolution using the FP technique by improving the recovery algorithm and setup modifications [9–15]. Besides using LEDs at large angles, an immersion medium can also be used to increase the  $NA_{illum}$ , such as an oil immersion condenser. This idea was demonstrated by using a planar LED configuration along with a condenser lens and an oil layer [16]. One disadvantage of using a condenser is that it should be precisely aligned with respect to the optical axis. In addition, a planar  $x - y$  LED board with constant spacing between LEDs is not the optimum choice [2]. To achieve a sufficient SNR, especially for the dark-field images, and to use minimum number of LEDs, a dome-shaped LED array is preferred over the planar LED board. LEDs installed in a dome have much lower power falloff for off-axis LEDs as compared to planar board [17]. There have been reports of implementations of the dome-LED illuminator [17, 18] and quasi-dome shaped LED [19, 20] configurations. In all these studies, since the electric wave is propagating in air ( $n = 1.0$ ), the  $NA_{illum}$  is restricted by the maximum illumination angle and large angles are needed to achieve high illumination NA. One alternate solution to increase  $NA_{illum}$  is to replace the in-between medium with a higher refractive index material ( $n > 1.0$ ). In our work, an oil-filled dome is designed and built that is filled with ordinary cooking oil with  $n = 1.465$ . As such this scheme is a cost-effective and fast FP setup that provides higher  $NA_{illum}$  without increasing the number of LEDs or maximum illumination angle. This paper is organised as follows: Section 2 covers the FPM theoretical background. Its hardware implementation in a dome LED array in air and when filled with oil is discussed in Section 3. The FPM recovery results are summarised and compared, followed by the discussion of future work and the conclusion.

**Theoretical background and FPM setup:** A schematic diagram of the proposed FPM setup is given in Figure 1. It includes a 3D printed dome-shaped LED array controlled by a programmed Arduino board. LEDs with central operation wavelength  $\lambda$  are implemented in the specific

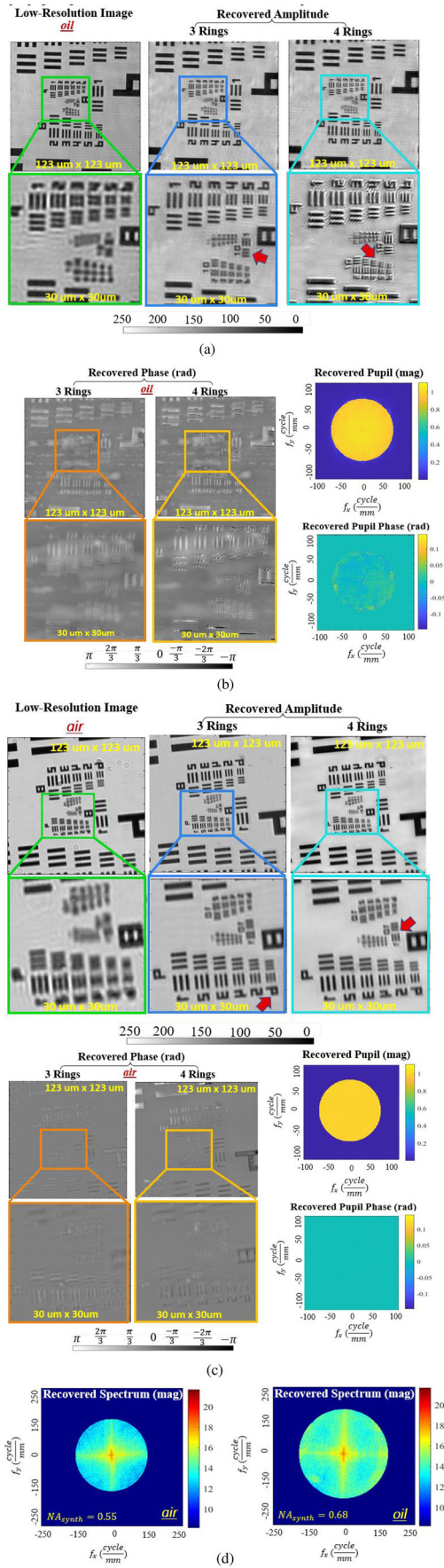


**Fig. 2** FPM recovery for the USAF amplitude test target target. (a) Recovered amplitude, oil-filled dome. (b) Recovered phase and pupil function, oil-filled dome. (c) Recovered amplitude, phase and pupil function in the free space propagation (empty dome) and (d) recovered frequency spectrum for the HR image. The resolved USAF elements are indicated by red arrows

positions related to the polar angle  $\theta$  and azimuthal angle  $\phi$  defined in the spherical coordinate system. Assuming that each LED is quasi-monochromatic and spatially coherent, it illuminates the sample at a specified angle. Based on the Fourier optics [1], multiple illumination angles contribute to a shift in the object spectrum and an extended transfer function beyond the cut-off frequency of the objective lens is obtained. The plane wave propagated by  $n$ th LED within the array can be described by  $\exp(jk_n \cdot r)$  in which  $k_n$  corresponds to the oblique illumination from the  $n$ th LED. The incident plane wave interacting with the thin specimen of interest is modelled as the transmission matrix  $\bar{O}(r) \exp(jx \frac{2\pi}{\lambda} \sin(\theta_x), jy \frac{2\pi}{\lambda} \sin(\theta_y))$  which is transformed to the Fourier plane under incident angles of  $\theta_x$  and  $\theta_y$ .

The coherent transfer function (CTF) of the diffraction-limited optical system, termed pupil function  $P(k_x, k_y)$  in the spatial domain, is multiplied to the complex object in the Fourier domain as

$$I = \left| \text{FFT}^{-1} \left[ P(k_x, k_y) \text{FFT} \left( \bar{O}(x, y) \exp \left( jx \frac{2\pi}{\lambda} \sin(\theta_x), jy \frac{2\pi}{\lambda} \sin(\theta_y) \right) \right) \right] \right|^2$$

$$= \left| \text{FFT}^{-1} \left[ P(K_x, K_y) \bar{O} \left( k_x - \frac{2\pi}{\lambda} \sin(\theta_x), k_y - \frac{2\pi}{\lambda} \sin(\theta_y) \right) \right] \right|^2, \quad (1)$$

wherein the captured LR intensity image is  $I$ ,  $P(k_x, k_y)$  is the pupil function and the object spatial spectrum is  $\bar{O}(k_x, k_y)$ . The HR complex image is recovered by performing a sequentially updating cycle based on propagating the field to the image plane, substituting the propagated field amplitude with the LR captured image, propagating it back to the Fourier plane and substituting the appropriate sub-spectrum; this cycle is repeated until the convergence criterion is satisfied [3]. The unknown pupil aberration in the objective lens is also digitally estimated and corrected during the recovery procedure, thus compensating for optical aberrations to produce a highly resolved HR image. According to the theory of FPM, the spatial resolution is selected to be  $\delta_x$ . To avoid sampling artifacts and aliasing, the maximum frequency in the calculated spectrum should be less than  $1/(2\delta_x)$  according to the Nyquist criterion [21]. To remove any out-of-band spurious signals and any undesired frequency content beyond the half-sample frequency value, the pixel size of the LR matrix image should be less than  $\lambda/(2 NA_{obj})$  and similarly the pixel size of the HR matrix image has to be less than  $\lambda/(2 NA_{synth})$ . Consequently, the maximum spatial frequency reached by  $f_{max, synth} = NA_{synth}/\lambda$ . It is worth mentioning that to achieve good convergence of the FPM recovery, the object spectrum overlap between adjacent rings should be higher than 50% [22]. Here, the dome array is designed with densely spaced LEDs in the central rings and more sparsely arranged towards the outer rings. This configuration results in a minimum number of LEDs needed to achieve a certain synthetic NA by keeping a constant spectral overlap between adjacent LEDs, in contrast to the planar LED board where the spectrum overlap increases for LEDs at larger incidence angles thus resulting in a lot more LEDs than needed. In addition, in the planar LED board, the LEDs at large angle shine much less light on the sample, thus degrading the SNR for the dark-field images which leads to a poor FPM recovery.

**Recovery from experimental images in air and oil medium: comparison and discussion:** This section is devoted to verifying the FPM scheme using a series of LR experimental images from USAF 1951 test target (*Ready Optics*) which provides a standard resolution measurement. The FPM setup employs an objective lens (10X,  $NA_{obj} = 0.28$ ) and a digital camera (Basler acA5472-17 μm, 5496 × 3672 pixels count) with 2.4 μm pixel size. Here, the dome LED array was used to illuminate the specimen at the central wavelength  $\lambda = 530$  nm. As a means of increasing the  $NA_{illum}$ , the dome was filled with an oil that has a refractive index of 1.465 and oil was directly in contact with the sample glass slide. To demonstrate the advantage of oil immersion over free space, LR images were first captured using an empty dome, and then the dome was filled with the oil. After capturing sequential images by four rings (37 total LEDs) to reconstruct the HR image, an LR matrix size 512 × 512 pixels



**Table 1. Theoretical and experimental comparison of FPM setups in free space ( $n = 1.000$ ) and oil ( $n = 1.465$ ) for LEDs on the dome (3 and 4 rings) with  $NA_{obj} = 0.28$ ,  $\lambda = 530$  nm**

Medium	3 Rings LEDs		4 Rings LEDs	
	air	oil	air	oil
Theoretical resolution (nm)	576	482	482	390
Measured Resolution (nm)	548	488	488	345
$NA_{illum}$	0.18	0.27	0.27	0.40
$NA_{synth} = (NA_{obj} + NA_{illum})$	0.46	0.55	0.55	0.68

of central patch was selected and the HR up-scaling ratio was set to 8. For the oil-filled dome, the  $NA_{illum}$  equalled 0.40, resulting in  $NA_{synth} = 0.68$ . As the CCD pixel size is  $2.4 \mu\text{m}$  in the Basler camera, the pixel size on the sample plane is  $0.24 \mu\text{m}$ . The HR image consisting of  $4096 \times 4096$  pixels was obtained with a good convergence of the recovery algorithm after 20 iterations. Theoretically, the half-pitch resolution defined as  $\delta r = 0.5\lambda / NA_{synth}$  is expected to be 390 nm and 482 nm for oil and air media, respectively.

The recovered high-resolution complex images after executing the FPM algorithm are presented in Figure 2, for both oil-filled medium and free-space propagation, considering results for three and four rings. The cut-off frequency for the oil system was slightly above the USAF target element 4 of group 10, resulting in a resolved resolution of 345 nm. Using the oil, resolution provides an appreciable gain over the raw LR images, especially when employing the images corresponding to the fourth ring. In comparison, the resolution of 488 nm (group 10, element 1) was achieved for the air system with four rings. Similarly, the results for three rings in air show that group 9, element 6 with 548 nm resolution was resolved. In addition, the recovered pupil magnitude and phase and the recovered object spectrum are shown in Figure 2. It clearly shows the benefits of the oil-filled setup with higher  $NA_{synth}$ , illustrating a wider frequency spectrum recovery. A summary of the comparison between the FPM recovery in the free-space propagation and the oil filled media using three and four rings is presented in Table 1. It is worth mentioning that the sample was held by a sample holder that does not allow any gaps between the oil and the sample slide.

**Conclusion:** This paper presents the results of FPM imaging using an oil-filled dome-shaped LED array. In this study, the dome utilised four rings with in total only 37 LEDs thus reducing the number of acquired captured images, resulting in both fast image capturing and reconstruction. The FPM recovery was examined in two different ways: first, the dome was not filled and light propagated in free space, and then dome was filled with oil. In the latter case, we achieved a higher resolution and wide FOV due to increased synthetic NA (from 0.55 in air to 0.68 in oil). Compared to the FPM with the incoming light propagating in air, the oil medium can enhance the spatial resolution from 488 nm (air) to 345 nm (oil). With this concept validated, our FPM with the oil-filled dome can be applied for the dome for complex specimens, such as biological samples and pathological applications. In the future, we plan to employ more rings in the dome in order to push the synthetic NA beyond unity with a minimum number of LEDs.

**Acknowledgements:** This work was supported by the Research Council of Norway through its CoE funding scheme (PoreLab, project number 262644) and NANO2021 (project number 272248), and KD PhD scholarship (project number 2700114).

**Conflict of interest:** The authors declare no conflicts of interest.

**Data Availability Statement:** Data supporting the findings of this study are available from the corresponding author, Mahdiah Gholami Mayani, upon reasonable request.

© 2022 The Authors. *Electronics Letters* published by John Wiley & Sons Ltd on behalf of The Institution of Engineering and Technology.

This is an open access article under the terms of the Creative Commons Attribution License, which permits use, distribution and reproduction in any medium, provided the original work is properly cited.

Received: 2 April 2022 Accepted: 9 June 2022

doi: 10.1049/ell2.12596

## References

- Goodman, J.W.: *Introduction to Fourier Optics*. 4th ed. W.H. Freeman Macmillan Learning, New York, NY (2017)
- Zheng, G., Horstmeyer, R., Yang, C.: Wide-field, high-resolution Fourier ptychographic microscopy. *Nat. Photonics* **7**(9), 739–745 (2013)
- Zheng, G.: *Fourier Ptychographic Imaging*. Morgan and Claypool Publishers, San Rafael, CA (2016)
- Tian, X.: Fourier ptychographic reconstruction using mixed Gaussian-Poisson likelihood with total variation regularisation. *Electron. Lett.* **55**(2), 1041–1043 (2019)
- Hasanzade, M., Hussain, N., Breiby, D.W., Akram, M.N.: Fourier ptychography algorithm based on scaled Fourier transform. *Electron. Lett.* **57**(3), 123–125 (2021)
- Hoshi, I., Kakue, T., Ito, T., Shimobaba, T., Wagatsuma, Y., Yamamoto, Y.: Phase retrieval using axial diffraction patterns and a ptychographic iterative engine. *Appl. Opt.* **59**(2), 354–362 (2020)
- Đuriš, M., Chmelík, R.: Super-resolution in coherence-controlled holographic microscope using synthetic aperture approach. OSA Optical Sensors and Sensing Congress 2021 (AIS, FTS, HISE, SENSORS, ES) (2021), paper JTU5A21 JTU5A.21 (2021)
- Dan, D., Lei, M., Yao, B., Wang, W., Winterhalder, M., Zumbusch, A., et al.: DMD-based LED-illumination super-resolution and optical sectioning microscopy. *Sci. Rep.* **3**(1), 1–7 (2013)
- Bian, L., Suo, J., Situ, G., Zheng, G., Chen, F., Dai, Q.: Content adaptive illumination for Fourier ptychography. *Opt. Lett.* **39**(23), 6648–6651 (2014)
- Zhou, A., Lee, B., Lam, E.Y., Situ, G., Chen, N., Wang, W.: Fast and robust misalignment correction of Fourier ptychographic microscopy for full field of view reconstruction. *Opt. Express* **26**(18), 23661–23674 (2018)
- Aldabbagh, A., Hasanzadeh, M., Breiby, D.W., Akram, M.N.: Fourier ptychographic imaging using a high numerical aperture dome illuminator. *Frontiers in Optics/Laser Science*, paper JTh4B28 JTh4B.28 (2020)
- Wang, C., Zhang, J., Yang, L., Sun, P., Wu, R., Tao, X., et al.: Forward imaging neural network with correction of positional misalignment for Fourier ptychographic microscopy. *Opt. Express* **28**(16), 23164–23175 (2020)
- Konda, P.C., Loetgering, L., Zhou, K.C., Xu, S., Harvey, A.R., Horstmeyer, R.: Fourier ptychography: current applications and future promises. *Opt. Express* **28**(7), 9603–9630 (2020)
- Sun, M., Li, Y., Huang, G., Wang, J., Tan, J., Liu, S., et al.: Self-adapting search algorithm for Fourier ptychographic microscopy. *Opt. Quantum Electron.* **53**(12), 1–13 (2021)
- Wang, D., Wang, D., Han, Y., Zhao, J., Zhao, J., Rong, L., et al.: Enhanced image reconstruction of Fourier ptychographic microscopy with double-height illumination. *Opt. Express* **29**(25), 41655–41669 (2021)
- Sun, J., Zuo, C., Zhang, L., Chen, Q.: Resolution-enhanced Fourier ptychographic microscopy based on high-numerical-aperture illuminations. *Sci. Rep.* **7**, 1–11 (2017)
- Pan, A., Zhang, Y., Wen, K., Zhou, M., Min, J., Lei, M., et al.: Sub-wavelength resolution Fourier ptychography with hemispherical digital condensers. *Opt. Express* **26**(18), 23119–23131 (2018)
- Phillips, Z.F., D'Ambrosio, M.V., Tian, L., Rulison, J.J., Patel, H.S., Sadras, N., et al.: Multi-contrast imaging and digital refocusing on a mobile microscope with a domed led array. *Plos One* **10**(5), 1–13 (2015)
- Phillips, Z.F., Eckert, R., Waller, L.: Quasi-dome: a self-calibrated high-NA LED illuminator for Fourier ptychography. *Imaging Appl. Opt.* **2017**, IW4E.5 (2017)
- Eckert, R., Phillips, Z.F., Waller, L.: Efficient illumination angle self-calibration in Fourier ptychography. *Appl Opt* **57**(19), 5434–5442 (2018)
- Konda, P.C.: Multi-Aperture Fourier Ptychographic Microscopy: development of a high-speed gigapixel coherent computational microscope. PhD Dissertation, University of Glasgow (2018)
- Liu, Q., Kuang, C., Fang, Y., Xiu, P., Li, Y., Wen, R., et al.: Effect of spatial spectrum overlap on Fourier ptychographic microscopy. *J. Innovative Optical Health Sci.* **10**, (2016)